Optics Letters

Diode-side-pumped continuous wave $Nd^{3+}:YVO_4$ self-Raman laser at 1176 nm

Cristine Calil Kores,[1,*] Jonas Jakutis-Neto,[2] Dimitri Geskus,[3] Helen M. Pask,[4] and Niklaus U. Wetter[1]

[1]Centro de Lasers e Aplicações, IPEN-CNEN/SP, Av. Professor Lineu Prestes, 2242, São Paulo (SP), Brazil
[2]Instituto de Estudos Avançados—IEAv, 12228-001 São José dos Campos (SP), Brazil
[3]Department of Materials and Nano Physics, KTH-Royal Institute of Technology, Kista 16440, Sweden
[4]MQ Photonics, Department of Physics and Astronomy, Macquarie University, Sydney, NSW 2109, Australia
*Corresponding author: nuwetter.ipen@gmail.com

Received 27 March 2015; revised 7 July 2015; accepted 7 July 2015; posted 8 July 2015 (Doc. ID 236955); published 23 July 2015

Here we report, to the best of our knowledge, the first diode-side-pumped continuous wave (cw) $Nd^{+3}:YVO_4$ self-Raman laser operating at 1176 nm. The compact cavity design is based on the total internal reflection of the laser beam at the pumped side of the $Nd^{+3}:YVO_4$ crystal. Configurations with a single bounce and a double bounce of the laser beam at the pumped faced have been characterized, providing a quasi-cw peak output power of more than 8 W (multimode) with an optical conversion efficiency of 11.5% and 3.7 W (TEM_{00}) having an optical conversion efficiency of 5.4%, respectively. Cw output power of 1.8 W has been demonstrated.

OCIS codes: (140.3490) Lasers, distributed-feedback; (140.3550) Lasers, Raman; (140.3480) Lasers, diode-pumped; (190.2620) Harmonic generation and mixing.

http://dx.doi.org/10.1364/OL.40.003524

Raman lasers have proven to be practical, economical, and efficient devices that are very wavelength agile and permit access to many wavelengths across the visible and infrared [1,2]. The first Raman laser was demonstrated in 1963 [3], and it took until 2004 to demonstrate the first continuous wave (cw) laser operation of a solid-state Raman laser, pumped externally by an Argon laser [4]. The first intracavity cw Raman laser was reported in 2005 [5]: it was a diode-pumped device. The continuous improvements to coating and crystal growth technologies have significantly contributed to the development of practical and efficient, diode-pumped Raman lasers with low (few-Watt) thresholds and mW to multi-Watt output powers [6]. For example, a cw intracavity Raman laser was reported in 2009 having an output power of 3.36 W at 1180 nm using the crystal combination $Nd:YVO_4$ (fundamental)—$BaWO_4$ (Stokes), and yielding an optical conversion efficiency of 13.2% [7]. When combined with intracavity sum frequency generation, Raman lasers provide access to hard-to-reach visible wavelengths in the yellow to orange [8] and most recently the blue to green [1], serving applications in various areas, such as medicine, biomedicine, and remote sensing.

The most compact, simple, and low-cost Raman lasers are the self-Raman lasers, in which laser transition and stimulated Raman scattering (SRS) processes occur in the same crystal. The reduced number of optical components inside the cavity of a self-Raman laser reduces the intracavity losses, which is essential to reach higher laser efficiency as the optical gain provided by SRS is small, and fundamental wave intensity must be of the order of MW/cm^2. However self-Raman lasers also present essentially two disadvantages: first, there is no possibility to separately optimize the mode sizes in the laser crystal and in the Raman crystal in order to achieve the best mode coupling between the fundamental and Stokes fields; and second, in crystalline Raman lasers, the thermal load in the gain crystal is not only induced by the pump, but also induced by the inelastic scattering process that generates the Stokes wavelength. The combined thermal loads typically limit the powers obtainable from self-Raman lasers.

The $Nd:YVO_4$ crystal, proposed as a self-Raman medium in 2001 by Kaminskii *et al.* [9], has yielded Watt-level output powers. A maximum output power of 1.53 W, corresponding to an optical conversion efficiency of 6.8% at 1176 nm, was reported for a cw $Nd:YVO_4$ self-Raman laser [10]. The same group demonstrated an output power of 1.84 W, having an optical conversion efficiency of 7.8%, by using a composite crystal $YVO_4/Nd:YVO_4$ [11]. To date, the highest cw output power from an intracavity Raman laser was obtained in 2012 by Savitski *et al.*, having an output power of 6.1 W by using a KGW crystal pumped by a Nd:YLF module [12], corresponding to 4% optical conversion efficiency. However, the highest conversion efficiency for a cw Raman laser was obtained in 2007 by Lisinetskii *et al.* [13], with the crystal Nd:KGW/KGW, yielding the value of 14%.

In a diode-end-pumped configuration, power scaling is difficult because of the challenges of coupling of high-power pump beams to the TEM_{00} mode of the laser resonator,

0146-9592/15/153524-04$15/0$15.00

and managing the strong thermal lensing. In addition, increasing the power of fiber-coupled diode pump sources is typically accompanied by increased spectral bandwidth as well as an exponential increase in costs if reasonable beam quality is required. Also, fiber-coupled pump sources are generally not polarized which, in connection with birefringent gain media, may cause further overall efficiency loss. This makes the pump source an item of disproportional cost within the otherwise economical Raman laser device.

An alternative, cost-effective approach is to use a side-pumping scheme with grazing incidence geometry [14], in which the laser beam makes a total internal reflection at the pumped facet of the crystal. A Nd:YVO$_4$ laser based on this geometry, with single pass through the gain medium, has shown high output powers at 1064 nm and a slope efficiency of 74% [15]. Using a further refinement of this type of resonator, called double-beam-mode-controlling (DBMC) technology [16,17,18], the modal behavior inside the cavity can be controlled by changing the angle that the laser beam makes with the pump surface and the distance between the bounces of the two beams at the pumped surface, as shown in Fig. 1. By creating good overlap between the two laser beams and the pumped region, higher modes are prevented from oscillating, which allows for the generation of efficient, stable, and high-quality TEM$_{00}$ laser operation. It has been demonstrated that this side-pumped technology can be much more efficient than longitudinal pumping [19]. Given the high efficiency of DBMC and the cost-effectiveness of side-pumping, it is therefore of interest to investigate if this technology can be applied advantageously to intracavity-converted, solid-state Raman lasers.

Here we report for the first time, to our knowledge, a diode-side-pumped Nd:YVO$_4$ self-Raman laser providing continuous (cw), and quasi-continuous (QCW) laser emission at 1176 nm, using the single bounce grazing incidence configuration and DBMC technology. To minimize the thermal load of the crystal, we employed in-band pumping of the Nd:YVO$_4$ crystal at 880 nm instead of the traditional 808 nm pump wavelength [20].

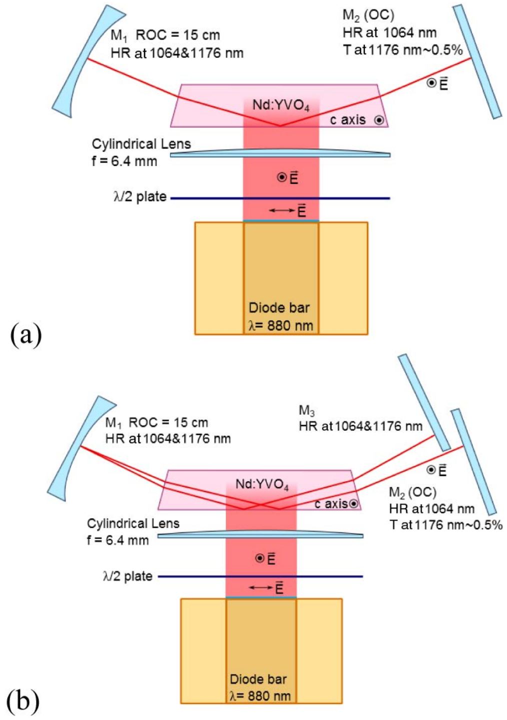

Fig. 1. Configuration of the laser setup with (a) single-bounce and (b) double-bounce geometry using DBMC.

The laser material used in our experiments was an a-cut Nd:YVO$_4$ crystal (Crystech) with 1.1 at. % Nd^{3+} doping concentration and dimensions of 22 mm × 5 mm × 2 mm, with the c-axis oriented perpendicular to the larger surfaces, as indicated in Fig. 1. The 5 × 2 mm facets had antireflection coating for 1064 and 1175 nm, cut at an angle of 5° to minimize possible parasitic self-lasing effects. The 22 × 5 mm pump surface was coated for high transmission at 808 and 880 nm. The crystal was mounted on a copper heat sink refrigerated by a recirculating chiller set to a temperature of 20°C. A 0.125-mm-thick indium foil was placed between the crystal and the holder to ensure optimal thermal contact. A 70-Watt TE-polarized diode bar (Jenoptik) was used as pump source, and its output wavelength was temperature tuned to 880 nm. An achromatic half-wave plate (Thorlabs) was used to control the polarization of the pump laser to address the crystal's π-polarization that has the highest absorption cross-section at 880 nm [21]. At this wavelength, 95% of the pump radiation gets absorbed in a thin layer at the pump facet of 400 μm. The pump laser diode bar was mounted onto a temperature-controlled copper plate, using indium foil for optimal thermal contact. A cylindrical lens with $f_v = 6.4$ mm was used to create a line focus with a height of 50 μm and a width of 11 mm at the crystal facet.

The 7-cm-long cavity used for the single bounce experiment, shown in Fig. 1(a) consisted of two mirrors M$_1$ (15-cm radius of curvature, $R > 99.99\%$ at 1064 and 1175 nm), and M$_2$ (plane, $R > 99.99\%$ at 1064 nm and transmission of $T = 0.47\%$ at 1175 nm). Figure 1(b) shows a schematic representation of the experimental setup used for the DBMC experiment, in which the cavity was 8.5 cm long. A third plane mirror (M$_3$) was added with the same coating as M$_1$. The TEM$_{00}$ fundamental mode size inside the DBMC (passive) cavity and the single-pass cavity were simulated using an ABCD matrix resonator model (LASCAD GmbH) providing a 150-μm beam diameter in the laser/Raman crystal; the mode size tended to decrease as the thermal lens increased, and the cavity remained stable for thermal lenses up to 50-mm focal length.

Both cw as well as the QCW laser performance were investigated using the single bounce geometry. Unfortunately, cw laser performance using the DBMC configuration could not be characterized because of catastrophic damage to the (unpumped) end of the Nd:YVO$_4$ crystal. In QCW operation, the pump was pulsed with a duty cycle of 0.3% at a repetition rate of 20 Hz, which corresponds to a pulse duration of 150 μs, approximately twice the lifetime of the upper laser level [22]. In this regime, we can assume that the laser dynamics are effectively cw, while thermal effects are negligible. A longpass filter (FEL1150 Thorlabs) was used to block the small residual output power of the fundamental laser at 1064 nm and to measure the 1st Stokes laser output power at 1176 nm.

First, the single-bounce geometry was explored in a multimode regime, which generated the highest Stokes powers.

Here, the large gain volume in the crystal allowed many high-order Gaussian–Hermite modes to oscillate. The laser delivered a maximum multimode QCW peak power of 8.4 W 1st Stokes at 1176 nm, corresponding to an optical-to-optical conversion efficiency of 11.7%. This is close to the highest efficiencies obtained for end-pumped intracavity Raman lasers [23]. A maximum QCW peak output power of 3 W was achieved when forcing the laser emission to TEM_{00} mode (purely by alignment of the resonator), corresponding to an optical conversion efficiency of 4.5%.

When applying the DBMC configuration, the laser mode size is decreased due to competition between the two beams in the gain medium, which favors TEM_{00} oscillation. This resulted in slightly improved laser efficiency in the QCW regime: the maximum Raman TEM_{00} QCW peak output power increased to 3.7 W, corresponding to an optical-to-optical conversion efficiency of 5.4%. As with the single-bounce configuration, no rollover in output power occurred, and the maximum output power was limited by the power available from the laser diode. The QCW laser performance for these various configurations is shown in Fig. 2.

The fundamental and Stokes output beam profiles have been recorded using a camera (Newport LBP-4-USB). A band pass filter (Newport FL 1064-10) was used to select only the fundamental field, and another band pass filter (Thorlabs FEL-1150-1V) was used to select only the Stokes field. Care was taken to ensure the camera was not saturated. The profiles reveal a strongly truncated fundamental, and a near-Gaussian Stokes, consistent with Raman beam cleanup, which is commonly observed in intracavity Raman lasers [24]. As an example, Fig. 3 shows beam profiles obtained using the DBMC configuration.

Cw operation of the Raman laser using the single bounce configuration delivered a maximum output power of 1.8 W at 1176 nm at the maximum pump power of 24.5 W, corresponding to an optical-to-optical conversion efficiency of 7.3%. The laser characteristic is shown in Fig. 4 (left). The maximum pump power was limited by the cw current that could be safely passed through the laser diode. For pump powers up to 8 W, the predominant laser mode oscillating was the TEM_{00} mode. For output powers of less than 100 mW, the Raman laser performance presented an irregular behavior, similar to observations made for a three-level Raman lasers in [25], and the threshold power was calculated by linear extrapolation.

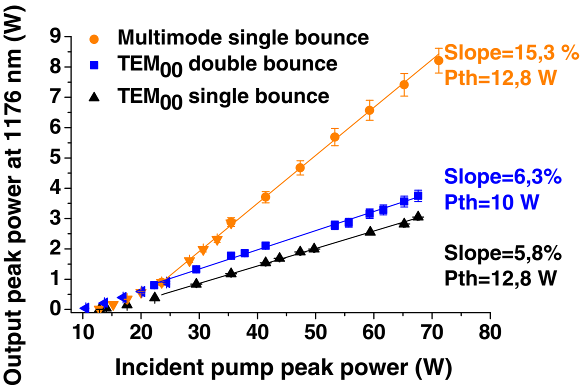

Fig. 2. QCW output power of lasers based on single-bounce, multimode operation; single-bounce, TEM_{00} operation; and with double-bounce, TEM_{00} operation.

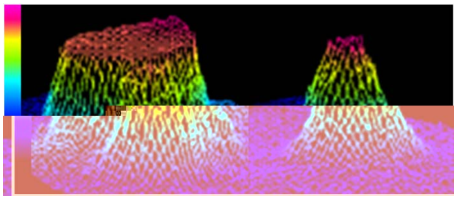

Fig. 3. Images of the fundamental laser beam (left) and the Stokes laser beam (right) from the DBMC laser.

The YVO_4 crystal has a positive thermo-optic coefficient (dn/dt); therefore, a strong positive thermal lens is expected for the cw self-Raman laser. Fortunately, the TEM_{00} mode is less affected by the thermal lens, due to its smaller size.

Measurements of the M^2 value of the output beam were made by using a lens to focus the beam, and translating a CCD camera through the focal plane. The highest beam quality was observed for cw pumping with 6 W of incident pump power in single-bounce configuration, where the beam quality in horizontal and vertical planes were $M_x^2 = 1.11$ and $M_y^2 = 1.01$. For the cw single bounce laser, pump powers above 8 W initiated oscillation of higher order Stokes modes, powered by multimode fundamental beams. The experimental data is shown in Fig. 4 (right). Measurements of the M^2 value for the QCW Raman output beam obtained with the DBMC configuration were performed, using the knife-edge method, and the obtained values were $M_x^2 = 1.32$ and $M_y^2 = 1.22$. The M^2 did not change with increased pump power, while the larger M^2 values of the single-bounce geometry ($M_x^2 = 1.77$ and $M_y^2 = 1.42$ for around 8-W pump power) were more sensitive to the mirror alignment and incident pump power.

In the DBMC experiment, the laser beam path through the crystal is two times longer than in the single-bounce configuration, providing twice the Raman gain, explaining the lower value of the threshold power (P_{th}) obtained using the DBMC configuration, as shown in Table 1. However, the losses also are doubled given that we have twice the number of crystal to air interfaces [18]; therefore, the slope efficiency remains virtually the same. A possible explanation for the lower threshold during

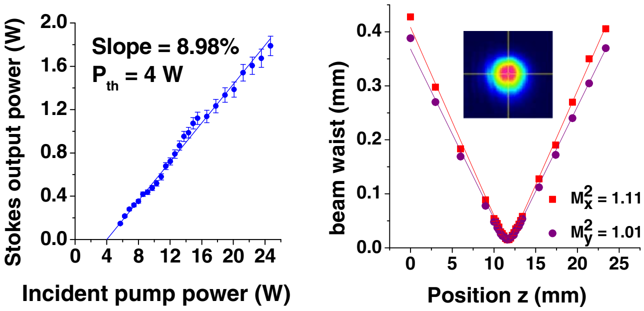

Fig. 4. Left: CW output power of the single-bounce configuration. Output is multimode for incident pump powers >8 W. Right: M^2 measurement of the cw Raman laser beam with single-bounce configuration, at a pump level of 6 W (inset: image of focus).

Table 1. Measured Laser Performances for the Laser Configurations Used in this Work

	M_x^2	M_y^2	P_{th}(W)	$P_{\max}$(W)	Optical Efficiency (%)
QCW single bounce (multimode)	—	—	12.8	8.4	11.7
QCW single bounce (TEM_{00})	1.77	1.42	12.8	3	4.5
QCW DBMC (TEM_{00})	1.32	1.22	10	3.7	5.4
CW single bounce (TEM_{00})	1.11[a]	1.01[a]	4	1.8	7.3

[a] Measured at 6 W of pump power.

cw operation (Fig. 4, left) when compared to QCW operation (Fig. 2) could be the observed longer buildup time of the Stokes field at low fundamental powers resulting in not enough time to completely build up the Stokes during the 150-μs-long pump pulse. Another explanation would come from the fact that in cw regime, the thermal load is higher creating a thermal lens that somehow is beneficial to the mode coupling. It needs further investigation in order to be conclusive.

Finally, we observed the typical blue luminescence mentioned in previous works using vanadate crystals as Raman active medium [26,27]. As studied by Jakutis-Neto *et al.* [28], this blue luminescence comes from Tm impurities and can have moderate influence for the thermal lensing and reducing laser output power. Especially for the DBMC configuration, the laser modes undergo more than 44 mm of crystal per pass, showing the blue emission all the way. However, the influence of the thermal load is negligible compared to the heat load deposited by the diode pump beam, and the extra losses are partially compensated by the extra gain due to the longer path inside the crystal.

We have demonstrated, to the best of our knowledge, the first cw laser operation of a side-pumped self-Raman laser. Using the grazing incidence geometry, we have characterized both single-bounce and DBMC configurations, providing a maximum QCW-multimode output power of 8.4 W at 1176 nm, corresponding to an optical efficiency of 11.7%. A maximum single-mode QCW output power of 3.7 W was obtained using the DBMC technology. The DBMC did not only demonstrate superior efficiency compared to the single-bounce geometry, but also provided a robust beam quality being insensitive for pump power variations and cavity alignment. Cw laser operation of the DBMC was not demonstrated due to a fracture in the crystal. Cw laser operation of the single-bounce geometry resulted in a multimodal output power of 1.8 W at 1176 nm, and fundamental transverse-mode laser operation was demonstrated at low pump levels. We anticipate that future cw laser operation of the DBMC technology will provide highly efficient laser emission with a robust beam quality.

We expect that this laser source will enable the development of economical, compact, high-power visible to infrared laser sources, when combined with nonlinear frequency doubling techniques.

Funding. Conselho Nacional de Desenvolvimento Científico e Tecnológico (National Council for Scientific and Technological Development) (2012 402241); Fundação de Amparo à Pesquisa do Estado de São Paulo (São Paulo Research Foundation) (2012 11437-8).

REFERENCES

1. D. Geskus, J. Jakutis-Neto, H. Pask, and N. Wetter, Opt. Lett. **39**, 6799 (2014).
2. J. Jakutis-Neto, J. Lin, N. Wetter, and H. Pask, Opt. Express **20**, 9841 (2012).
3. G. Eckhardt, D. P. Bortfeld, and M. Geller, Appl. Phys. Lett. **3**, 137 (1963).
4. A. S. Grabtchikov, V. A. Lisinetskii, V. A. Orlovich, M. Schmitt, R. Maksimenka, and W. Kiefer, Opt. Lett. **29**, 2524 (2004).
5. A. A. Demidovich, A. S. Grabtchikov, V. A. Lisinetskii, V. N. Burakevich, V. A. Orlovich, and W. Kiefer, Opt. Lett. **30**, 1701 (2005).
6. J. A. Piper and H. M. Pask, IEEE Sel. Top. Quantum Electron. **13**, 692 (2007).
7. L. Fan, Y. X. Fan, Y. Q. Li, H. Zhang, Q. Wang, J. Wang, and H. T. Wang, Opt. Lett. **34**, 1687 (2009).
8. A. Lee, D. Spence, J. Piper, and H. Pask, Opt. Express **18**, 20013 (2010).
9. A. A. Kaminskii, K. Ueda, H. J. Eichler, Y. Kuwano, H. Kouta, S. N. Bagaev, T. H. Chyba, J. C. Barnes, G. M. A. Gad, T. Murai, and J. Lu, Laser Phys. **11**, 1124 (2001).
10. H. Zhu, G. Zhang, Y. Duan, C. Huang, and Y. Wei, Chin. Phys. Lett. **28**, 054202 (2011).
11. H. Y. Zhu, Y. M. Duan, G. Zhang, C. H. Huang, Y. Wei, W. D. Chen, L. X. Huang, and Y. D. Huang, Appl. Phys. B **103**, 559 (2011).
12. V. Savitski, I. Friel, J. Hastie, M. Dawson, D. Burns, and A. Kemp, IEEE J. Quantum Electron. **48**, 328 (2012).
13. V. A. Lisinetskii, A. S. Grabtchikov, A. A. Demidovich, V. N. Burakevich, V. A. Orlovich, and A. N. Titov, Appl. Phys. B **88**, 499 (2007).
14. M. J. Damzen, M. Trew, E. Rosas, and G. J. Crofts, Opt. Commun. **196**, 237 (2001).
15. N. U. Wetter, F. A. Camargo, and E. C. Sousa, J. Opt. A **10**, 104012 (2008).
16. A. M. Deana, M. A. P. A. Lopez, and N. U. Wetter, Opt. Lett. **38**, 4088 (2013).
17. N. U. Wetter, E. C. Sousa, I. M. Ranieri, and S. L. Baldochi, Opt. Lett. **34**, 292 (2009).
18. A. M. Deana and N. U. Wetter, Appl. Phys. B **117**, 855 (2014).
19. N. U. Wetter and A. M. Deana, Laser Phys. Lett. **10**, 035807 (2013).
20. N. Pavel, V. Lupei, J. Saikawa, T. Taira, and H. Kan, Appl. Phys. B **82**, 599 (2006).
21. L. McDonagh, R. Wallenstein, R. Knappe, and A. Nebel, Opt. Lett. **31**, 3297 (2006).
22. L. Fornasiero, S. Kück, T. Jensen, G. Huber, and B. H. T. Chai, Appl. Phys. B **67**, 549 (1998).
23. V. A. Lisinetskii, A. S. Grabtchikov, I. A. Khodasevich, H. Eichler, and V. A. Orlovich, Opt. Commun. **272**, 509 (2007).
24. J. T. Murray, W. L. Austin, and R. C. Powell, Opt. Mater. **11**, 353 (1999).
25. D. Geskus, J. Jakutis-Neto, S.-M. Reijn, H. M. Pask, and N. U. Wetter, Opt. Lett. **39**, 2982 (2014).
26. H. Y. Zhu, Y. M. Duan, G. Zhang, C. H. Huang, Y. Wei, W. D. Chen, Y. D. Huang, and N. Ye, Opt. Lett. **34**, 2763 (2009).
27. W. Baoshan, T. Huiming, P. Jiying, M. Jieguang, and G. Lanlan, Opt. Mater. **29**, 1817 (2007).
28. J. Jakutis-Neto, C. Artlett, A. Lee, J. Lin, D. Spence, J. Piper, N. Wetter, and H. Pask, Opt. Mater. Express **4**, 889 (2014).